

MECHANISMS OF SEA-DEPTH CHANGES IN SILURIAN EPEIRIC BASINS OF EAST SIBERIA

E.V. Artyushkov and P.A. Chekhovich*

*United Institute of the Physics of the Earth, Russian Academy of Sciences,
10 ul. B. Gruzinskaya, Moscow, 123810, Russia*

** Lomonosov Moscow State University,
Vorob'yovy Gory, Moscow, 119899, Russia*

It is commonly recognized that sea level experienced strong global-scale systematic changes in the geologic past. Its 20–100 m fluctuations in 1–10 Myr (third-order) cycles are most often detected using Fischer plots based on thicknesses of meter-scale cycles in sections of shallow-marine carbonate facies. However, the classical Fischer plots constructed for different regions of East Siberia show considerable mismatch though eustatic changes are supposed to be globally synchronous. This mismatch is caused by time-dependent variations in durations of elementary cycles asynchronous in different sections. Therefore, a great number of earlier inferred global eustatic events apparently never existed in reality. We obtained more reliable accommodation plots with thicknesses of 0.5 Myr synchronous chronozones as elementary units in the Silurian sections of East Siberia. According to these plots, eustatic fluctuations never exceeded $\pm 5\text{--}7$ m throughout the Silurian, which is far below the accepted magnitude of 30–130 m. The Silurian stratigraphic subunits and intervals between tectonic events were constrained due to stable durations of the chronozones. Our plots reveal strong lateral variations of crustal subsidence rates over East Siberia. These variations were controlled neither by the flexural response of lithosphere to changes in horizontal stresses nor by the mantle topography dynamics, but rather by metamorphic phase change and related consolidation of the mafic lower crust. Subsidence rates occasionally became times faster or slower within ~ 0.5 Myr intervals, the contrasts surprisingly great for platforms. Phase change rates may have been controlled by deviatoric stresses in addition to temperature and fluid migration. This mechanism can be responsible for subsidence rate variations reported for many intracratonic basins.

Siberian craton, Silurian, epeiric seas, subsidence rate, metamorphism in lower crust, eustasy, sedimentary cycles

INTRODUCTION

Most of epeiric seas experienced repeated depth changes through their geologic history commonly attributed to eustatic fluctuations [1–3]. Regression-transgression cycles with magnitudes from 20 to 100 m and durations from 1 to 10 Myr called “third-order cycles” or “eustatic events” have received special attention. They are relevant to hydrocarbon exploration of sands deposited during regressions in emerged shelf and peritidal environments or of turbidites at the slope foot of paleo-basins [4], such as the Achimov member in West Siberia [5]. These events, assumed to be globally synchronous, are often used in correlations among geographically dispersed sections [6, etc.].

Water depths were noted to change also under the effect of tectonic uplift and subsidence [7, 8, etc.]. The existence of many eustatic events was doubted [9–11] for the lack of a satisfactory explanation for sudden rises and falls, except waxing and waning of large ice sheets which however have not been reliably documented over most of the Phanerozoic. Yet, periodic eustatic events are almost commonly accepted whereas the role of tectonic uplift and subsidence is confined to an additional complicating factor of paleo-depth changes [12, etc.].

Eustatic events were hypothesized for almost all Phanerozoic periods, e.g. 50–100 m events in Late Cambrian and earliest Ordovician inferred from sea-depth changes [13]. Rapid sea-level changes within ± 10 m distinguished in late Early Cambrian–middle Tremadoc (Early Ordovician) sections in East Baltica spanning about 45 Myr [14, 15] were likely caused by a tectonic mechanism.

Eight eustatic events [16] possibly reaching a magnitude of ~ 100 m [17] were suggested for Silurian epeiric basins on the basis of paleo-depth reconstructions. Evidence from the Silurian stratigraphy of East Siberia [18–20] and mathematical modeling of sea depths show that 1–3 Myr harmonic eustatic cycles as well as cycles with a sharp regression phase did not exceed 20–30 m [17]. We in this study estimate the maximum magnitude of sea-level fluctuations of arbitrary shapes and durations on the basis of recently published high-resolution Silurian sections [21]. We additionally improved the dating precision for some Silurian events and revealed significant changes in crustal subsidence rates in different parts of the East Siberian basin. The reported results have implications for the physical mechanism responsible for the apparent sea-level variations.

DETECTION OF EUSTATIC EVENTS USING FISCHER PLOTS

Use of Fischer plots is a classical guide to sea-level history [8, 22–25]. Sections of carbonate platforms deposited in shallow-marine environments at sea depths ≤ 5 –10 m [26] are stacked successions of meter-scale elementary cycles with durations from 0.01 to 1 Myr. Each cycle starts with steep rise followed by gradual recovery of the sea depth. Fischer diagrams are based on long successions of thicknesses of 1–10 Myr cycles corresponding to eustatic fluctuations, with the simplifying assumptions of (i) fixed cycle period, (ii) global synchronicity of cycles, and (iii) fixed crustal subsidence rates. The thickness of each cycle is taken relative to the mean thickness of sediments that would continuously fill up the accommodation space produced by subsidence at a fixed rate (line OO' in Fig. 1). The thickness of a cycle (AB) equal to the magnitude of subsidence (AC) in this cycle (Fig. 1, *a*) means that deposition keeps up with subsidence and the sea level is invariable; AB longer than AC (positive slope, Fig. 1, *b*) marks a thicker-than-average cycle and a sea-level rise for $CB = AB - AC$; AB shorter than AC (negative slope, Fig. 1, *c*) corresponds to a thinner-than-average cycle and a sea-level fall for BC . The point B of each cycle is added by the point O of the following cycle. The broken line that envelopes the peaks of cycles OB is believed to approximate slower third-order eustatic sea-level changes.

CLASSICAL FISCHER PLOTS FOR SILURIAN SECTIONS OF EAST SIBERIA

Silurian East Siberia was occupied by a large sea [21] (Fig. 2). In the earliest Silurian, peritidal deposition at sea depths 0–10 m occurred in its southern and southeastern parts (stratigraphic provinces (“districts” in [21]) 13, 14, and 15 in Fig. 2) and an outer shelf environment existed in the center and in the north. Deposition on the shelf had produced a peritidal environment over the greatest portion of the basin by the middle Silurian. The basin was dominated by a large carbonate platform (0–5 m) surrounded by a back-shoal lagoon (< 10 m). The upper section was eroded (Upper Silurian sediments in the south and uppermost Upper Silurian in the southeast).

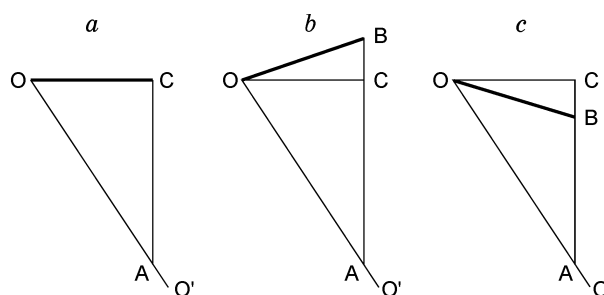


Fig. 1. Main types of meter-scale cycles in Fischer plots. Line OO' shows crustal subsidence at a constant rate. *a*: sea level remains invariable, and thickness of sediments AC that fill accommodation space equals magnitude of subsidence during a cycle. *b*: sea level rises for CB , and sediment thickness AB exceeds subsidence AC . *c*: sea level falls for CB , and sediment thickness AB is less than subsidence AC .

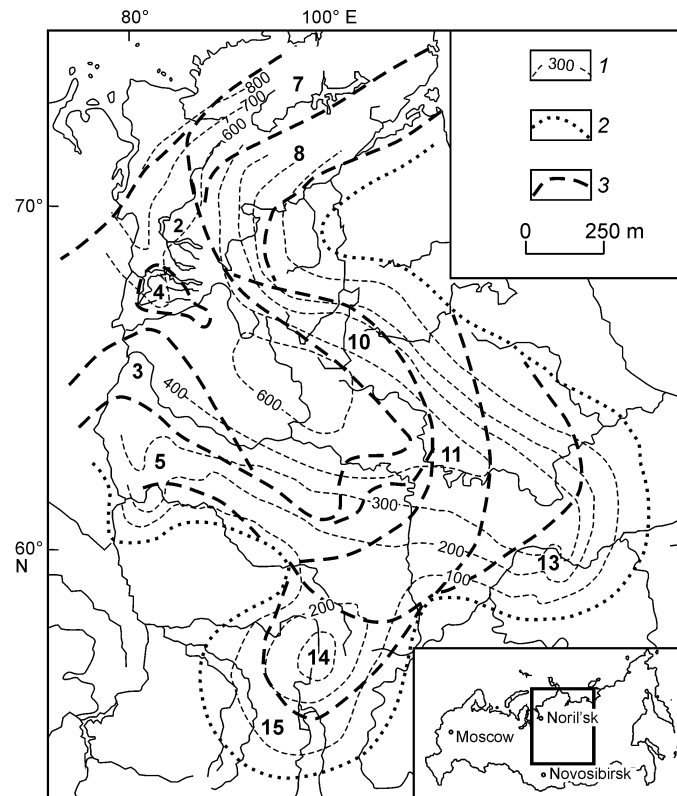


Fig. 2. Thickness of Silurian sediments in East Siberia (modified after [21]) and locations of documented stratigraphic provinces referred to in Figs. 3–5. Provinces are listed after [21] and coded by Arabic numerals as 2 — Norilsk, 3 — Turukhansk, 4 — Igarka, 5 — Kochumdek, 7 — South Taimyr, 8 — Ledyanka, 10 — Moyero, 11 — Morkoka, 13 — Nyuya-Berezovo, 14 — Ilimsk, 15 — Balturino; 1 — thickness contour lines (m); 2 — basin limits; 3 — province boundaries.

First we constructed classical Fischer plots for different stratigraphic provinces of East Siberia where shallow-marine environments persisted for a long time and peritidal carbonate facies are of broad occurrence (Fig. 3). The plots are based on successions of elementary cycle thicknesses for provinces 10, 11, and 13–15 documented to a high resolution [21], taking into account the now eroded sediment loads in provinces 10 and 11 [27]. The deviation of the plots from the x axis is commonly supposed to record eustatic sea-level changes. The cycles plotted episodes of sudden rise and fall (e.g., 30–40 m rise (EF) in plot 13 and (IJ) in plot 11; a 40 m fall for 5 Myr (GK), a 30 m rise for 2–3 Myr (KL) and a 20 m fall (MN) and a 35 m rise (NO) in plot 10; 50 m falls for 10 Myr (BH and AC) in plots 11 and 13).

Eustatic changes are globally synchronous and the respective Fischer plots are expected to be likewise similar. However, most falls and rises (Fig. 3) were asynchronous, i.e. two assumptions fail and the plots thus cannot represent eustatic changes. The cycle periods changed with time in each province (contrary to assumption 1): e.g., plot 11 shows 59 cycles in an 11 Myr interval spanning a great part of the Aeronian and Telychian [16, 28] and only 15 and 6 cycles, correspondingly, in the Wenlock (5 Myr) and Ludlow (4 Myr); the mean durations of the cycles are, respectively, 0.19, 0.33, and 0.67 Myr. This mismatch cannot be attributed to uncertainty in the duration of Silurian stratigraphic units.

Duration changes of real cycles cause much bias to the plots. Longer cycles look thicker (assuming fixed subsidence rates) and produce an upward shift of the plot which can be misinterpreted as a sea-level rise; shorter cycles produce a downward shift and can be in the same way misinterpreted as a sea-level fall.

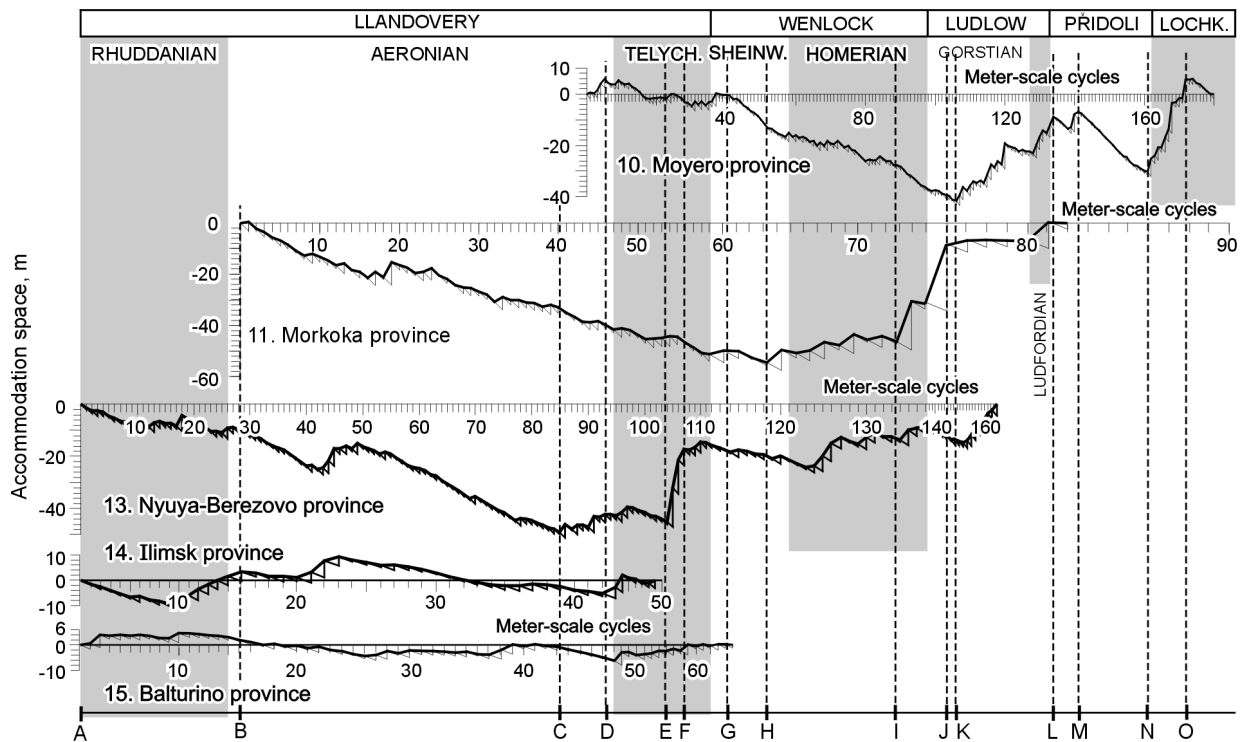


Fig. 3. Fischer plots for five provinces of Silurian East Siberian basin based on elementary cycles of carbonate facies, after data from [21]. For locations of provinces see Fig. 2. Plots of this type are often used to identify 1–10 Myr eustatic fluctuations (e.g., [23–25]) and include 1–4 Myr third-order and ≥ 10 Myr second-order cycles. Plots for different regions differ strongly from one another, namely, because of time- and space-variable durations of elementary cycles (see text). Therefore, these Fischer plots cannot reveal 1–20 Myr eustatic fluctuations.

Moreover, the cycle number for synchronous intervals varies geographically: e.g., 15, 25, and 62 cycles in the Wenlock in plots 11, 13, and 10, with their duration ratio 1:0.6:0.24.

Crustal subsidence rate varied in time and space contrary to assumption 3 (see below).

Thus the behavior of elementary cycles in the Siberian Silurian sections is consistent with none assumption implied in the classical Fischer plots as a guide to eustatic sea-level history.

Therefore, the Silurian deposition history of East Siberia which was typical of many epeiric seas makes doubt about the existence of many eustatic events inferred earlier for Phanerozoic sections from Fischer plots [8, 23–25, etc.].

FISCHER PLOTS BASED ON CHRONOZONE THICKNESSES

The Silurian section of East Siberia includes 54 regional lithostratigraphic units, called chronozones, corresponding to ~ 0.5 Myr time intervals [20, 21]. The basin always had good connection with ocean in the northwest (in the present frame of reference) and the chronozones have been reliably correlated to the standard international time scale on the basis of graptolite and conodont biozones (38 and 12 zones, respectively, in the Silurian section). We also used regional biostratigraphic scales based on hundreds species of corals, brachiopods, ostracods, and vertebrates. The resolution of the chronozone division in Silurian East Siberia is superior over many other basins worldwide and other time periods with 1–2 Myr or longer elementary units. Division into 0.5–1.0 Myr biozones [29] was achieved only for few sections elsewhere, e.g., in Middle and Upper Devonian Euroamerica [30] and lower Carboniferous Mississippi in North America [31], whereas the existence of numerous exposures in East Siberia provided reliable correlation of Silurian deposits over the $2 \cdot 10^6$ km² basin.

The duration of Silurian chronozones, or rather their time equivalents (0.5 Myr), is comparable to the duration

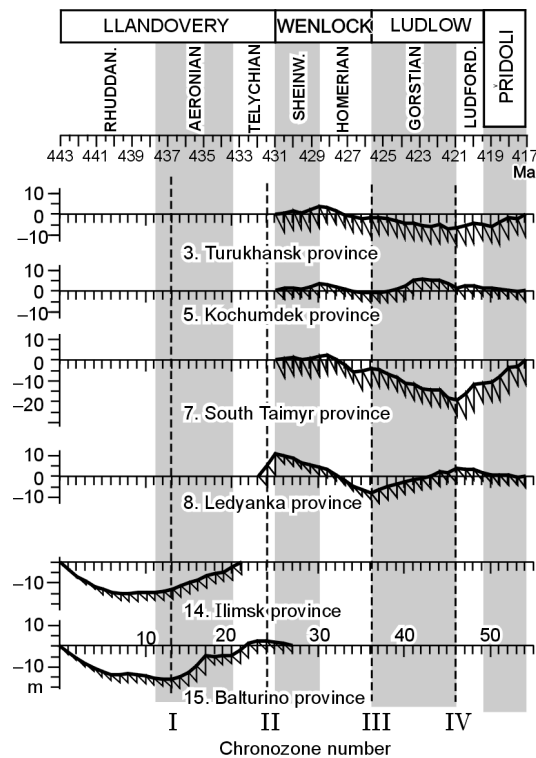


Fig. 4. Fischer plots for provinces 3, 5, 7, 8, 14, and 15 of Silurian East Siberian basin. For locations of provinces see Fig. 2. Plots are based on thicknesses of chronozones in Silurian peritidal facies synchronous for all provinces. Deviations from x axis do not exceed 5–15 m, therefore, no significant sea-level change occurred.

of 0.1–1.0 Myr elementary cycles in Fischer plots. Thus we obtained plots based on thicknesses of chronozones (Δh_{chr}) [20] deposited in peritidal environments. Plots 3, 5, 7, 8, 14, 15 (Fig. 4) show ≤ 10 –15 m deviations from the x axis; deviations in plots 2, 4, 10, 11, and 13 (Fig. 5) reach 30–80 m. Plots 14 and 15 are given for comparison in Fig. 5.

RELATIVE STABILITY OF THE SILURIAN EUSTATIC SEA LEVEL

Plots 3 and 5 (Fig. 4) in the Wenlock-Pridoli show fluctuations of relative sea level within 5–7 m which, in the common interpretation of Fischer plots, would be attributed to almost constant crustal subsidence rate and eustatic fluctuations within 5–7 m. Assume that the sea level at that time experienced high rises and falls almost cancelled by slower and faster subsidence, so that plots 3 and 5 remain nearly horizontal. Global eustatic fluctuations and regional tectonic movements are independent processes and would hardly balance each other in provinces 3 and 5 located 400 km apart. Moreover, plots 8 and 7 depart from the x axis for ± 10 and 17 m, respectively (Ledyanka province, 1000 km far to the north and Taimyr province, 1300 km far from 5). Therefore, eustatic fluctuations cannot be cancelled by crustal subsidence or uplift and did not exceed 5–7 m in Wenlock and Pridoli time. The deviations of plots 3 and 5 from the x axis can be attributed to eustatic fluctuations or to changes in crustal subsidence rate, and the eustatic fluctuations thus may have been still lower.

Plot 14 in Fig. 4 covers most of the Llandovery (Rhuddanian, Aeronian, and earliest Telychian), 12 Myr in total, and plot 15 spans the Llandovery and the earliest Wenlock (16 Myr). The two plots are rather similar over the interval from 1 to 21 chronozones and both show a 15 m fall in the latest Rhuddanian-earliest Aeronian. The common interpretation would infer a 15 m lower sea level, which is however disproved by comparison with plot 13 (Fig. 5). Its deviation within chronozones 1–21 has the same shape but a three times greater magnitude than in plots 14 and 15, whereas all would be identical were they of eustatic origin. Thus, the cycle thicknesses must have

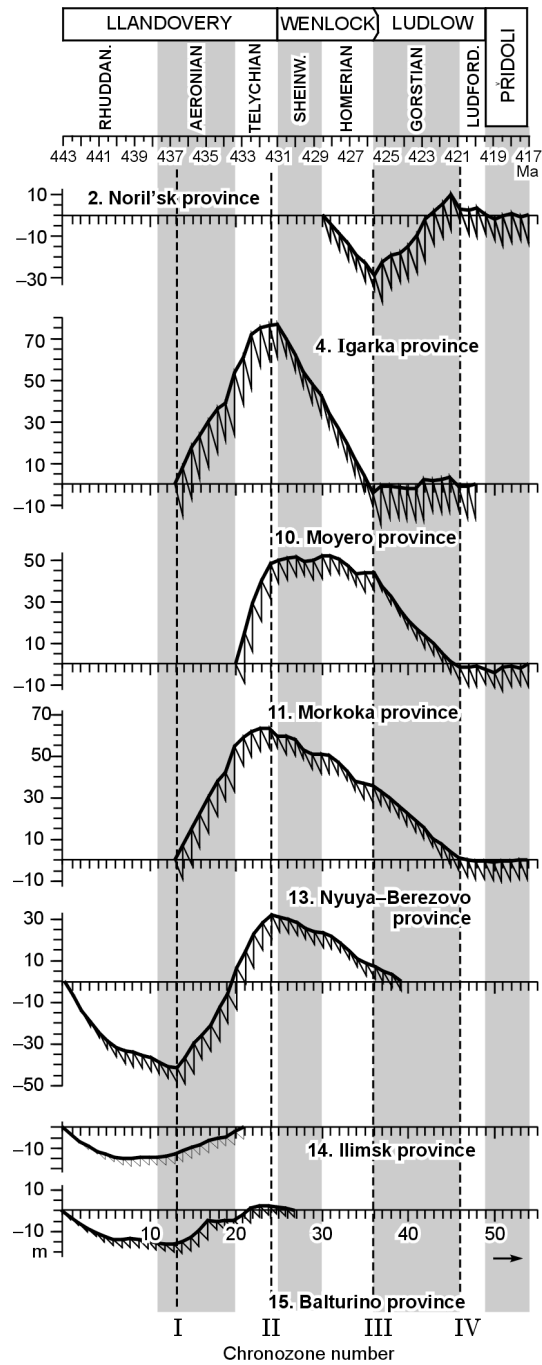


Fig. 5. Fischer plots for provinces 2, 4, 10, 11, and 13–15 of Silurian East Siberian basin. For locations of provinces see Fig. 2. Plots are based on thicknesses of chronozones in Silurian peritidal facies synchronous for all provinces. Most plots (provinces 2, 4, 10, 11, and 13) show significant deviations from *x* axis. At almost invariable eustatic sea level, rising portions of plots indicate faster-than-average and falling portions slower-than-average subsidence. Rises and falls in plots 14 and 15 with relatively small deviations from *x* axis are also mainly caused by variations in subsidence rate. Intervals of faster and slower subsidence are synphase to a first approximation but differ in magnitude.

been additionally controlled by tectonic movements at variable rates, and plots 13–15 can, in principle, record the composite signal of eustasy and tectonics.

Eustatic fluctuations and regional tectonic movements, being independent, should have different periodicities. They have comparable magnitudes in plots 14 and 15 but are out of phase with plot 13. Eustasy is likely responsible for a smaller part of deviation in 14 and 15, i.e., the sea-level change can be <5 m. Thus, sea-level changes in the Silurian remained within 5–7 m, which is much less than 30–130 m expected [17] from water-depth changes in other basins [16].

Small deviations from the x axis occur in other plots as well (Fig. 5): in 2, 10, and 11 over the Late Ludlow and the Pridoli (chronozones 46–54, ~3 Myr) and in 4 over almost the entire Ludlow (chronozones 36–48, ~4 Myr); plot 7 (Fig. 4) is nearly horizontal in the first half of the Wenlock (chronozones 26–31, 2–3 Myr). This is additional evidence for small eustatic fluctuations in Wenlock-Pridoli time.

QUASI-PERIODICITY OF CHRONOZONES IN THE WENLOCK-PRIDOL

Plots in Figs. 4 and 5 are constructed under the assumption of constant chronozone periods Δt_{chr} : $\Delta t_{\text{chr}} = \Delta t_{\text{chr}}^0$. However, Δt_{chr} may have varied with time as in classical meter-scale cycles, and the plots in Figs. 4 and 5 would be thus invalid for estimating eustatic fluctuations. Therefore, we are to estimate Δt_{chr} variations. The accommodation space associated with subsidence at a rate a within the intervals plotted in Figs. 4 and 5 was continuously filled with sediments. The thickness of a chronozone at invariable sea level is

$$\Delta h_{\text{chr}} = a \Delta t_{\text{chr}} \quad (1)$$

Let a be constant and Δt_{chr} change for a value $\delta(\Delta t_{\text{chr}})$: $\Delta t_{\text{chr}} = \Delta t_{\text{chr}}^0 + \delta(\Delta t_{\text{chr}})$. Then, the thickness Δh_{chr} changes as (Fig. 6, *a*):

$$\delta(\Delta h_{\text{chr}}) = a \delta(\Delta t_{\text{chr}}). \quad (2)$$

The elementary plots are based on the assumption of constant $\Delta t_{\text{chr}} = \Delta t_{\text{chr}}^0$ (Fig. 6, *b*), and crustal subsidence for the time Δt_{chr} is assumed equal to $a \delta(\Delta t_{\text{chr}}^0)$. In reality, the chronozone thickness changes for $a \delta(\Delta t_{\text{chr}})$ because Δt_{chr} changes for $\delta(\Delta t_{\text{chr}})$, and this biases the elementary plot (Fig. 6, *b*). Plots 3 and 5 in the Wenlock-Pridoli interval are almost horizontal. Such small deviation from the x axis at significant changes of Δt_{chr} can be provided only by simultaneous sea-level compensation:

$$\delta \zeta_{\text{eus}} = -a \delta(\Delta t_{\text{chr}}). \quad (3)$$

In this case, changes in chronozone thickness (2) due to increase or decrease in Δt_{chr} are balanced, respectively, by sea-level fall or rise. This inverse correlation between eustatic sea-level changes and the duration of regional chronozones in a basin with very shallow paleo-depths is very unlikely. Nevertheless, it is worth special consideration.

Thickness change $\delta(\Delta h_{\text{chr}})$ (2) is proportional to the subsidence rate a . At a given $\delta \zeta_{\text{eus}}$, (3) fulfils only at $a = a_0 = |\delta \zeta_{\text{eus}}| / |\delta(\Delta t_{\text{chr}})|$ when the elementary plot remains horizontal (Fig. 6, *c*). Thickness increment or decrement (2) exceeds the sea-level change $\delta \zeta_{\text{eus}}$ where $a > a_0$ (Fig. 6, *d*) and is less than $\delta \zeta_{\text{eus}}$ where $a < a_0$ (Fig. 6, *e*). The rate a is geographically variable: The difference is almost two-fold in provinces 3 and 5 where the plots of Fig. 4 are nearly horizontal (17.3 and 9.3 m/Myr, respectively). In these conditions, the horizontal position of both plots 3 and 5 cannot be provided by a $\delta \zeta_{\text{eus}}$ compensation of Δt_{chr} .

Plots 7 and 8 (Fig. 4), 2, 4, 10, and 11 (Fig. 5) include horizontal segments in Late Silurian intervals as well, which lends support to the absence of large Δt_{chr} changes, given a rate contrast of 9.3 m/Myr in 5 against 31.7 m/Myr in 4.

In the Llandovery, peritidal deposition at 5–10 m sea depths was restricted to some part of the basin. Early and Middle Llandovery sediments are preserved only in provinces 13–15, and the Late Llandovery is covered completely only in plots 4, 11, 13, and 15. Plots 14 and 15 are nearly horizontal within chronozones 7–13 and 20–22 where the subsidence rate a is roughly constant and the Δh_{chr} and, hence, Δt_{chr} changes are weak. Fischer plots are linear, though not necessarily horizontal, if Δt_{chr} and a remain constant over more than one chronozone, and show linear rise and fall in intervals with higher and lower a , respectively (e.g., Early Silurian intervals in plots 4, 10, 11, and 13). At a closer examination, Δt_{chr} appears quasi-constant in the Llandovery, at least since

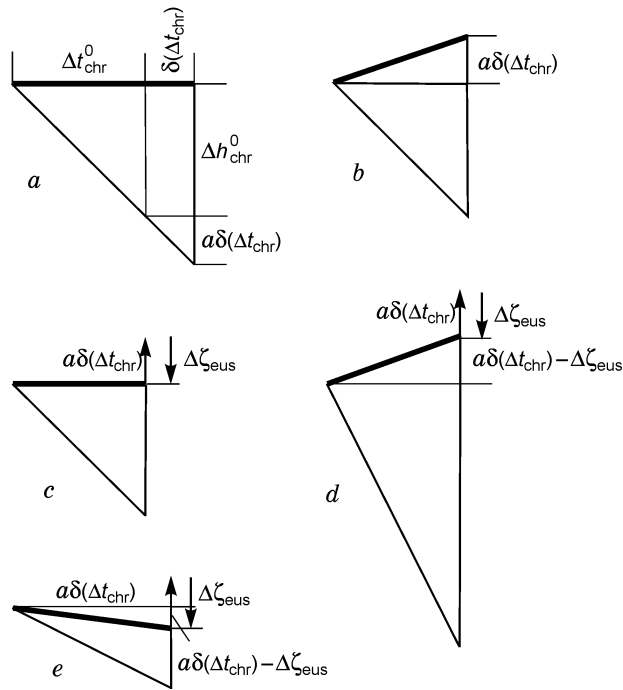


Fig. 6. Effect of $\delta(\Delta t_{\text{chr}})$ changes in duration of chronozones on Fischer plots based on Δh_{chr} thicknesses at fixed subsidence rate. *a* — increase $\delta(\Delta t_{\text{chr}})$ in Δh_{chr} caused by longer Δt_{chr} at invariable sea level; *b* — corresponding rise in plot based on assumption of fixed Δt_{chr} , i.e., without regard to $\delta(\Delta t_{\text{chr}})$ increase; *c* — compensation of this rise by synchronous sea-level fall for $\Delta \zeta_{\text{seus}} = -\delta(\Delta t_{\text{chr}})$ where subsidence rate $a = a_0 = |\Delta \zeta_{\text{seus}}| / |\delta(\Delta t_{\text{chr}})|$; *d* — rise associated with this sea-level change for an area with faster subsidence $a > a_0$; *e* — fall for area with $a < a_0$.

chronozone 7. Standard deviation of Δt_{chr} from the average did not exceed 10% within chronozones 7–13 and 3% within chronozones 14–22.

DURATION OF MAIN SILURIAN STRATIGRAPHIC UNITS

Boundaries between stratigraphic units are commonly constrained using isotope methods [32], which are however not very accurate. Absolute ages and durations of stratigraphic units can differ significantly in different time scales. The Silurian in Gradstein and Ogg's time scale [28] lasts 26 Myr (443–417 Ma) and the Wenlock, the Ludlow, and the Přidoli are, respectively, 5, 4, and 2 Myr; the Llandovery is 15 Myr. The Rhuddanian, Aeronian, and Telychian subunits have no absolute age constraints but their 4, 6.9, and 4.1 Myr durations, respectively, are inferred from a tentative duration ratio of 1:1.725:1.025 [16].

As shown above, Δt_{chr} varied weakly except for the earliest Llandovery. The time scale in Figs. 4 and 5 is based on the assumption of fixed Δt_{chr} (0.48 Myr) in the Silurian. This approach was used to estimate the durations of Silurian stratigraphic units and subunits as: 12.5, 5.3, 4.3, and 4.1 Myr for Llandovery, Rhuddanian, Aeronian, and Telychian, respectively (against the above estimates of 15, 4, 6.9, and 4.1 Myr); 5.3, 6.3, and 2.4 Myr, respectively, for Wenlock, Ludlow, and Přidoli (against 5, 4, and 2 Myr according to [28]); and 2.4, 2.9, 4.8, and 1.5 Myr, respectively, for Sheinwoodian, Homerian, Gorstian, and Ludfordian (subunits of Wenlock and Ludlow). The same approach yielded more accurate timing of intervals between individual events.

TIME-DEPENDENT CHANGES OF SUBSIDENCE RATES

The 30–80 m deviations in plots 2, 4, 10, 11, and 13 (Figs. 1, 5) were caused mainly by variations in crustal subsidence rates. The rising portions of the plots correspond to faster subsidence and higher sedimentation rates,

and slower subsidence associated with thinner cycles is marked by falls. Subsidence rates (a) varied significantly in space and time. The average subsidence rate in province 11 was 31.6 m/Myr in the Aeronian (chronozones 14–20) and 11.1 m/Myr, or 2.8 times as low, in the Gorstian (chronozones 37–47); in province 4 it was 20.7 m/Myr in the Telychian (chronozones 21–25) and 7.8 m/Myr, or 2.7 times as low, in the Wenlock (chronozones 26–36).

The plots contain 4–6 Myr nearly horizontal or linearly dipping segments where subsidence rates are almost invariable. Horizontal segments correspond to subsidence rates about the regional average, positive slope to faster-than-average and negative slope to slower-than-average subsidence. Rises and falls notably correlate in different provinces. Plots 4, 10, 11, and 13 show a rise in the middle and late Llandovery. Slow subsidence occurred in provinces 7 (Fig. 4), 11 and 13 (Fig. 5) over the greatest part of the Wenlock–Prídoli interval. In provinces 4, 11, and 13 a fall started almost simultaneously in latest Telychian. Subsidence in provinces 8 (Fig. 4), 4, and 2 was slow in the Wenlock and fast in the Ludlow (Fig. 5).

MECHANISM OF GENERAL CRUSTAL SUBSIDENCE

The thickness of the Silurian section in East Siberia reaches 600–800 m (Fig. 2), or far in excess of 30–80 m rises and falls (Fig. 5) associated with faster or slower subsidence. Rate oscillations only complicated the general subsidence while the latter required contraction of the lithosphere in the absence of its significant extension and far from collision belts. Crust and mantle density can increase by cooling [34, 35] but this mechanism works only in regions where lithospheric heating occurred at least 100 Myr ago. The Silurian cratonic lithosphere in Siberia was about 1 b.y. old [36, 37] and cooled long ago. Therefore, lithospheric cooling cannot contribute much to subsidence, and more so, cannot be responsible for its rate variations within 1–10 Myr intervals far shorter than the characteristic time of lithospheric thermal relaxation $t_{tl} \sim 100$ Myr.

The 600–800 m thick Silurian marine facies in East Siberia make up only a small portion of the 10–12 km sedimentary section [38, 39]. They mostly deposited upon cold Late Proterozoic lithosphere long before the eruption of Triassic flood basalts. Consolidation of mafic lower crust by metamorphic phase change from gabbro to garnet granulites appears the only plausible mechanism for the deep subsidence of cold lithosphere [40–43] and the only candidate to provide the general crustal subsidence in the Silurian. Below we consider what may have been the cause of rapid variations in subsidence rate.

FLEXURAL RESPONSE OF LITHOSPHERE TO CHANGES IN HORIZONTAL STRESSES

The flexural response of lithosphere [44–45] with a laterally variable thickness [46, 47] to changes in horizontal stresses is an often invoked driving mechanism of its vertical movements. Flexure is necessary to balance the torque of additional forces that act along lithospheric plates. The departure of cratonic lithosphere from isostasy is usually as small as ≤ 100 –200 m, and its vertical displacement related to the above mechanism is as a rule within this magnitude. The amount of displacement is inversely proportional to the square width (L) of the thickness anomaly $\zeta \sim 1/L^2$ [46, 47], and significant displacement is thus restricted to 300–500 km wide regions, which is often neglected. Let, for instance, the effective elastic thickness of lithosphere (H_y) vary along the x axis as (Fig. 7)

$$H_y = (H_y)^0 + \Delta H_y \sin(\pi x/L), \quad (4)$$

where $(H_y)^0$ is the mean lithospheric thickness in a region. Let in-plane forces change for $\Delta\Sigma$. Then, the deflection of sediment-loaded lithosphere from its initial position is given by [15]

$$\zeta \sim \zeta_0 \sin(\pi x/L), \quad (5)$$

$$\zeta_0 = \pi^2 \Delta\Sigma \Delta H_y / [2(\rho_m - \rho_{sed})gL^2], \quad (6)$$

where ρ_{sed} is the sediment density, $\rho_m = 3350 \text{ kg/m}^3$ is the mantle density, $g = 9.81 \text{ m/s}^2$ is the gravity acceleration. The elastic thickness of Precambrian cratonic lithosphere (H_y) is 70–90 km [48, 49], and its lateral variations in Silurian East Siberia hardly exceeded $2\Delta H_y \sim 20$ –30 km, or $\Delta H_y \sim 10$ –15 km. The characteristic scale of in-plane forces Σ applied to plates is comparable to mean pressure from spreading ridges on the adjacent oceanic plates $\Sigma_{char} \sim 2 \cdot 10^{12} \text{ N/m}$ [50]. If the change Σ was about Σ_{char} or $\Delta\Sigma \sim 2 \cdot 10^{12} \text{ N/m}$, with the width of the East Siberian basin $L \sim 1200 \times 2000 \text{ km}$, and $\rho_{sed} = 2500 \text{ kg/m}^3$, (6) gives

$$\zeta_0 \sim 3\text{--}12 \text{ m}, \quad (7)$$

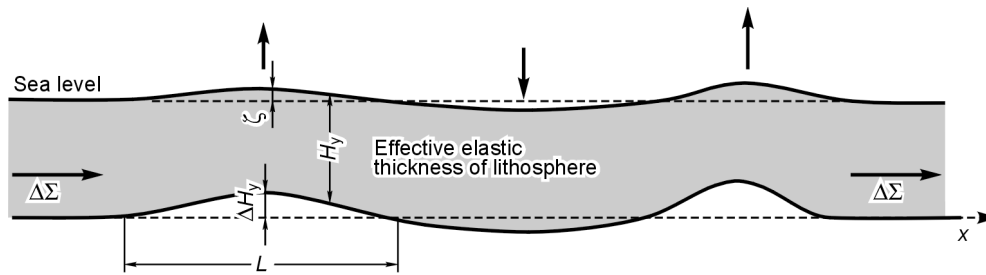


Fig. 7. Deformation of lithospheric layer of laterally variable thickness H_y in response to additional in-plane forces $\Delta\Sigma$.

which is much less than the 30–80 m rises and falls in plots 2, 4, 10, 11, and 13 in Fig. 5. Therefore, this mechanism appears inapplicable to East Siberia as a whole. However, the effective elastic thickness of the lithosphere may have changed in a more complicated way. If high- and low- H_y regions alternated, the size L of H_y anomalies was times smaller than the basin width. Since $\zeta_0 \sim 1/L^2$, the amount of vertical displacement was an order of magnitude greater than (7) and comparable to rises and falls in the plots of Fig. 5.

Assume that variations in subsidence rate v_1 were caused by flexural response of the lithosphere to changes in horizontal stresses and overprinted uniform subsidence at a mean rate of v_0 . The total subsidence rate $v = v_0 + v_1$ varied with time, and v_1 was thus comparable to v_0 . Then, upward v_1 may have occasionally exceeded downward v_0 . In peritidal environments this would cause uplift and emergence of sediments above the sea-level whereby the section would miss some chronozones. However, the sections plotted in Figs. 4 and 5 are complete, i.e., eleven geographically dispersed regions of East Siberia experienced long-lasting subsidence at a variable rate rather than uplift. Thus subsidence rate variations hardly can have been driven by lithospheric flexure.

Moreover, rises and falls in plots 2, 4, 10, 11, and 13 locally have the same slopes, i.e., vertical deflection from uniform subsidence varied at a constant rate. If this deflection was caused by changes in the forces Σ , they would increase or decrease almost linearly over long intervals ($d\Sigma/dt \approx \text{const}$) and $d\Sigma/dt$ would abruptly change in sign at kinks. It is difficult to figure out processes on plate boundaries to explain this peculiar behavior of Σ .

VARIATIONS IN MANTLE DYNAMIC TOPOGRAPHY

Mantle convection causes vertical deflection of the asthenospheric top from the equilibrium (the so-called dynamic topography [51]) and related deflection of the overlying lithosphere. This can be, for instance, due to mantle flow over subducting oceanic plates. The position of collision boundaries and subduction dip control the flow pattern, and flow intensity is proportional to subduction rate. Moreover, the elastic flexure of continental plates increases with age because of load buildup from tectonic nappes, sediments, and volcanics.

These effects were hypothesized to produce 10–100 Myr cycles of paleo-depths [52]. In the Silurian, subduction occurred south of East Siberia (in the present frame of reference) [53], and subsidence, in principle, can have been generally uniform but overprinted by time-dependent rate changes associated with the dynamics of the subduction regime. Subducting plates most often dip at 40–50°, and mantle flow over them covers an area up to 600–800 km. Thus the subduction-related mantle flow would be able to reach northern East Siberia located over 2000 km far from the collision boundary only if the plates subducted at $\leq 20^\circ$, which is rather unlikely.

Deflection of the lithosphere by mantle dynamic topography is difficult to estimate because of uncertainty in variable mantle viscosity (it can vary laterally for at least one order of magnitude), position of collision front, subduction rate and dip, and surface loads. Anyway, this deflection should decrease away from the collision boundary, which is not the case in East Siberia. In the Llandovery (Fig. 5) subsidence rate variations in the basin center (provinces 4, 10, 11, and 13, Fig. 2) at 1300 to 1800 km away from the zone of collision were times as great as in the south (provinces 14 and 15) 500–800 km far from the collision boundary. In Wenlock-Pridoli time, subsidence rates varied strongly in provinces 2, 4, 10, 11 and 13 located 1300 to 1800 km away from the collision zone but remained almost invariable in provinces 5 and 3 at a comparable distance (1100 and 1400 km) from there. Thus, the mantle dynamic topography associated with subduction beneath Siberia from the south did not cause any notable effect on subsidence, even if the subducting plate underlay a large part of the basin.

Moreover, mantle dynamic topography, including that related to small-scale convection, would produce

hiatuses in sedimentary sections [52], like the lithospheric flexure in response to in-plane forces. The absence of deposition gaps in Silurian East Siberia thus rules out both mechanisms.

Yet uplift and subsidence driven by mantle dynamic topography and elastic flexure of lithosphere may have occurred in other regions and in other periods. The latter mechanism should be tested as to the width of the uplift zone. Thermal relaxation of lithosphere may cause subsidence in basins which underwent heating of crust and mantle not long ago.

RAPID SUBSIDENCE OF CRATONIC CRUST

Subsidence in intracratonic basins resulting from metamorphic phase change in the lower crust [40–43, etc.] is most often slow (10–100 m/Myr) and continues hundreds of millions of years or longer, whereby the subsided basins accumulate 5 to 15 km of shallow-marine sediments. Or it can occasionally accelerate and produce, in ~1 Myr, deep seas in place of shallow shelf or lowland areas, such as the Late Jurassic West Siberian basin or the earliest Late Devonian Timan-Pechora, Volga-Ural, and Caspian basins.

The rate of phase change is commonly considered to be controlled by temperature (T) and water-bearing fluids [54, 55]. It increases with temperature by an order of magnitude at every 100 °C and grows abruptly in the presence of even minor amounts of water-bearing fluids. The origin of fluids in the lower crust is often attributed to dissolution of water-bearing minerals on heating in the basaltic layer [55, 56], which requires higher heat flux from the asthenosphere. This, however, cannot account for rapid subsidence in 1 Myr, extremely short compared to the characteristic time of thermal relaxation of cratonic lithosphere ($T_{tr1} \sim 100$ Myr).

Another explanation invokes upward migration of fluids from small mantle plumes [42, 57]. Rising plumes impinged on the lithospheric base are marked by swelling and magmatism on the surface, often preceding rapid subsidence. For instance, the Timan-Pechora basin developed on the eastern margin of a 1400 km wide swell [58] associated with numerous occurrences of magmatism, including kimberlite-pyrite and other alkali-ultramafic intrusions in the center (Archangelsk diamond province), ultramafic plutonism in the Kola peninsula and outpourings of flood basalts in the Timan region. Almost synchronous swelling of large areas indicates very low viscosity of plume heads and their sublithospheric spreading for ~1 Myr [59, 60].

The supply of mantle fluids into the lower crust in regions of rapid subsidence is confirmed by isotope evidence [61–63]. The Volga-Ural and Timan-Pechora basin fill contains high and strongly variable (contrasts up to six orders of magnitude) concentrations of Se, As, Mo, Hg, U, and Re, which is often explained by adsorption of these elements in layers rich in non-oxidized organic matter [64, etc.]. However, these high concentrations are encountered in both high- and low-organic layers, i.e., the adsorption effect is ruled out. Moreover, Nd and Sr isotope ratios in oil and bitumen from the same basins ($\epsilon_{Nd} = -9 \dots -12$, $^{87}Sr/^{86}Sr = 0.708-0.719$) are similar to those in Australian diamond-bearing lamproites [65], and this similarity was attributed to the effect of upward fluid migration from the mantle. Migration of asthenospheric fluids was also invoked [62–63] to explain extremely high contents of U in carbonates accumulated during Early Carboniferous rapid subsidence of the Caspian basin, an order of magnitude in excess of the typical for marine carbonates [66].

Diffusion of volatiles in the mantle is commonly very slow. An asthenospheric fluid can rapidly penetrate into the crust through mantle lithosphere if it reduces free energy on grain boundaries [67] and wets them as a surfactant [68]. Then, the fluid, which is under the same pressure as the host rock, easily percolates between crystals as a thin film ($10^{-5}-10^{-6}$ cm).

Rapid subsidence in East Siberia in the earliest Silurian produced a ≥ 100 m deep sea for 1 Myr in its central and northern parts in place of land [21]. This transgression could be accounted for by melting of an ice sheet which existed in the Southern Hemisphere in the Late Ordovician [69]. The southern and southeastern parts of the earliest Silurian basin (provinces 13, 14, and 15, Fig. 2) were areas of slow continuous peritidal (at ~10 m) deposition and bears no signature of significant eustatic sea-level rise. So, the ice sheet must have melted before.

Note that no laboratory experiments on low-temperature phase change from gabbro to eclogite are known. The Rebinder effect in mafic and ultramafic rocks also remains unexplored experimentally. Thus the composition of surface-active fluid carried into the lower crust by mantle plumes is unknown. Petrological data on exposures of voluminous high-grade mafic rocks rather concern the roots of Precambrian mountains dragged out to the surface than the cratonic lower crust. Therefore, we used mainly geological and geochemical evidence for the relationship between rapid subsidence and eclogitization in the lower crust associated with migration of surface-active fluids from mantle plumes, sufficient to identify the mechanism. This approach resembles that used to estimate mantle viscosity from data on postglacial isostatic rebound [47, etc.] and turned to be more efficient than laboratory experiments and theoretical considerations.

POSSIBLE MECHANISM OF RATE CHANGES IN SLOW SUBSIDENCE OF EAST SIBERIAN BASIN

The earliest Silurian rapid subsidence was followed by slow subsidence at a mean rate of 10–30 m/Myr. Mean subsidence rate v_0 is recorded in Fischer plots (Fig. 1) as the slope ratio of OO' corresponding to the falling portions of plots in Figs. 4 and 5 within each chronozone. Plots 2, 4, 10, 11, and 13 (Fig. 5) show large slope ratios and high v_0 : 25.5, 31.7, 18.4, 18.8, and 15.8 m/Myr, respectively. The same plots deviate strongly from the x axis, i.e., the variable component of subsidence rate, v_1 , is twice v_0 or more. In plots 5, 8, 14, and 15 (Fig. 4), v_0 is lower: 9.3, 10.3, 8.7, and 8.4 m/Myr, respectively, and v_1 and v_0 are often correlated. This indicates that subsidence rate variations must have been controlled by variations in phase change rate responsible for general crustal subsidence.

Subsidence under the load of sediments with the density ρ_{sed} and the thickness h_{sed} requires phase change to garnet granulites of gabbro with the density ρ_{gb} and an initial thickness

$$h_{\text{gb}} = (\rho_{\text{gl}}/\rho_{\text{m}}) [(\rho_{\text{m}} - \rho_{\text{sed}})/(\rho_{\text{gl}} - \rho_{\text{gb}})]h_{\text{sed}}, \quad (8)$$

where ρ_{gl} is the density of garnet granulites and $\rho_{\text{m}} = 3350 \text{ kg/m}^3$ is the mantle density. With $\rho_{\text{gb}} = 2950 \text{ kg/m}^3$, $\rho_{\text{gl}} = 3400 \text{ kg/m}^3$, and $\rho_{\text{sed}} = 2500 \text{ kg/m}^3$, the load of the 300–800 m Silurian section corresponds to phase change of a 600–1500 m thick gabbro layer. Additional 30–80 m subsidence would require consolidation of 60–150 m thick gabbro. It appears much more likely that subsidence was caused by weak consolidation in a thick layer. Assume that the density ρ_{gl}^0 of a h_{gl}^0 granulite layer reached ρ_{gl}^1 . Then

$$h_{\text{gl}}^0 = (\rho_{\text{gl}}^1/\rho_{\text{m}}) [(\rho_{\text{m}} - \rho_{\text{sed}})/(\rho_{\text{gl}}^1 - \rho_{\text{gl}}^0)]h_{\text{sed}}. \quad (9)$$

Let h_{gl}^0 be 10 km and $\rho_{\text{gl}}^0 = 3350 \text{ kg/m}^3$. Silurian sediment-loaded subsidence under $h_{\text{sed}} = 0.3\text{--}0.8 \text{ km}$ and $\rho_{\text{sed}} = 3500 \text{ kg/m}^3$ requires a density increase of $\rho_{\text{gl}}^1 - \rho_{\text{gl}}^0 = 26\text{--}69 \text{ kg/m}^3$ (0.08–0.2% of ρ_{gl}^0).

What can be the cause of variations in phase change rate? Episodes of rapid and slow phase change are reflected in the rising and falling portions of plots (Figs. 4 and 5) equated to 5 to 7 Myr with ~0.5 Myr transition from one to another. The alternation was hardly caused by temperature change in the lower crust which cannot be so abrupt. Therefore, fluid release by dissolution of water-bearing minerals on heating in the lower crust is improbable.

The earliest Silurian rapid subsidence of the basin central and northern parts resulted from upward migration of fluid from a small mantle plume. Episodes of rapid subsidence are most often brief (~1 Myr) and their end means that the fluid migrated from the lower into the upper crust and sediments or became bound in water-bearing minerals. After sediments had filled up the initial depression, it became an area of slow and continuous peritidal deposition. The absence of deposition gaps indicates the absence of swelling, even as small as ~10 m, i.e., no more plumes rose to the lithospheric base. Nevertheless, subsidence rates strongly varied with time, in the north and center as well as on the basin periphery (provinces 13–15, Fig. 5) not subject to rapid subsidence and fluid migration effects in the earliest Silurian. Provinces 13–15 experienced rapid subsidence in Aeronian and Telychian time (see the rises in their plots in Fig. 5) as well as provinces 4, 10, and 11 where fluid from the mantle plume penetrated into the crust. Therefore, the phase change rate was controlled by some factor other than fluid migration.

Explanation can be found on closer examination of plots in Figs. 4 and 5. They contain 4–6 Myr segments of approximately constant slope corresponding to subsidence at a nearly constant rate v . At some levels v changed for 0.5 Myr simultaneously in several provinces (see kinks in the plots). In the Early Aeronian (level I), v increased abruptly in province 13. Since that time, v likewise became times as high for 2 Myr in province 15, 1100 km far from province 13 (Fig. 2), but remained almost invariable in province 14 located between 13 and 15, closer to province 15 (Fig. 2). At level II (latest Llandovery), v fell abruptly in provinces 4, 10, 11, and 13 (Fig. 5) and 8 (Fig. 4), almost simultaneously over a ~1700 km wide area (Fig. 2). At the Wenlock-Ludlow boundary, v decreased abruptly in province 10 (Fig. 5), increased in provinces 8 (Fig. 4), 2, and 4 (Fig. 5), and changed weakly in provinces 3, 5, and 13. Then subsidence slowed down at the Gorstian-Ludfordian boundary (level IV) in provinces 2 and 8 but accelerated in provinces 7, 10, 11, and changed little in provinces 3 and 5.

The variations were thus rather intricate, especially, at levels III and IV when subsidence accelerated or slowed down in different provinces and remained almost invariable in provinces 3 and 5, in the time when the temperature and fluid content could not change. Horizontal deformation of the lithosphere which affects the rate of metamorphism [70, 71] was insignificant on the cold craton. Only crustal stress may have experienced rapid

strong changes under the effect of additional forces [72, 73] whose magnitude and direction changed from time to time over large areas [74, etc.]. The rate of metamorphic phase change from gabbro to eclogite may have changed together with deviatoric stresses during their reorganization. This hypothesis is supported by synchronicity of rapid subsidence rate changes at levels I-IV in geographically distant regions.

Phase change in cold cratonic lower crust is very slow. Its kinetics and the very phase diagram have never been studied experimentally. Therefore, the effect of deviatoric stresses on phase change rate requires special consideration with reference to data from the theory of metals. It is known that the influence of deviatoric stresses on concentration of a new phase in alloys is an order of magnitude stronger than from bulk compression [75]. The behavior of reaction rate under stress change was not tested but the rate quite probably can increase with stress. Deviatoric stresses may influence the gabbro-eclogite phase change rate and also fluid migration. Even a "dry" lower crust can contain minor amounts of fluid under the same pressure as the host rock, which allows the fluid easily to migrate along cracks [76]. This mechanism can drive phase change in the rocks that remained unmetamorphosed.

DISCUSSION AND CONCLUSIONS

Paleozoic, Mesozoic, and Cenozoic epi-eric seas experienced periodic depth changes of a magnitude from 20 to 100 m and a duration from 1 to 10 Myr (third-order cycles) [1–3]. These sea-depth changes, which occurred also in the Silurian [16], are most often attributed to eustatic fluctuations [1–3, 16, etc.]; some workers accept regional tectonics as an additional factor. A few publications [e.g., 11, 77] express doubt about the existence of many global eustatic events, because the precision of the available age methods (≥ 1 Myr for the Paleozoic) is insufficient to constrain the synchronicity of ~ 1 Myr cycles in geographically dispersed regions, or because eustatic and tectonic signals cannot be yet convincingly separated.

Eustatic signals are often picked using Fischer plots [22–25] for successions of meter-scale cycles in peritidal (≤ 5 –10 m water depths) carbonate facies. The plots that record global eustasy are expected to be geographically uniform but the plots of Silurian elementary cycles constructed for various stratigraphic provinces of East Siberia turned to be different (Fig. 3), because the basic assumptions of the method failed.

The origin of higher-order sea-level cycles has received much attention [78–81, etc.]. They are commonly interpreted in terms of eustasy and a relationship to Milankovitch cycles [12, 81]. Then, they should be globally synchronous to provide correlation among distant regions as an essential clue to geochronology and petroleum exploration targets. Different durations of the elementary cycles in East Siberia and their geographic asynchronicity indicate that the cyclic structure of the sections is produced by non-eustatic processes such as discontinuity of deposition [78, 79, 82] or brief tectonic episodes like the instrumentally measured recent crustal movements [83, 84]. Our results show that many Phanerozoic global eustatic events inferred earlier from Fischer plots [23, 25, etc.] never existed in reality.

We constructed Fischer accommodation plots using the thicknesses of ~ 0.5 Myr chronozones, regional stratigraphic units distinguished in the Silurian peritidal section of the East Siberian basin [20, 21]. The plots for these synchronous intervals (Figs. 4 and 5) differ strongly from the classical Fischer plots (Fig. 3) based on cycles of uncertain durations. Some chronozone-based accommodation plots show small deviations from the x axis. This can be interpreted as almost constant subsidence rates and eustatic sea-level fluctuations within ± 5 –7 m. The Cambrian and earliest Ordovician eustatic fluctuations were shown before to be within ± 10 m [14, 15], the magnitude comparable to the Silurian fluctuations and far lower than 20–100 m suggested for third-order cycles [1–3, 16, etc.]. Therefore, the eustatic sea-level fluctuations had been apparently almost negligible within 1–10 Myr intervals since the earliest Paleozoic, except for large glaciations.

The available absolute age methods are of insufficient accuracy to constrain the durations of Silurian chronozones in East Siberia. Comparison of our accommodation plots for regions with different subsidence rates showed surprising stability of chronozone durations over the Silurian. This made a basis for a new Silurian time scale (Figs. 4 and 5, on top) which, unlike the common time scale [28], provides much more accurate timing for the durations of Silurian stratigraphic units and intervals between tectonic events.

The plots based on chronozone thicknesses record the deviation of crustal subsidence rates from the constant mean. These rates show abrupt changes within 0.5 Myr intervals, unexpected for a stable cratonic zone. Rapid changes were reported from other intracratonic basins as well [85] and their origin is of special interest. They are often explained in terms of flexural response of lithosphere to additional in-plane forces [e.g., 44, 45] or subduction-related mantle dynamic topography [52, etc.]. However, these mechanisms would from time to time cause uplift and emergence of the territory above sea level, which is inconsistent with the evidence of continuous carbonate deposition and persistent subsidence, though at a variable rate, in Silurian East Siberia.

Subsidence rates varied especially strongly in regions of generally faster subsidence. Therefore, their variations were most likely associated with the same process that drove general crustal subsidence. The 600-800 m subsidence of the East Siberian basin on a cold Precambrian craton can have been provided only by metamorphic phase change in the lower crust from gabbro to denser garnet granulites or eclogites.

The phase-change rate grows rapidly with temperature and increases abruptly in the presence of even minor amounts of water-bearing fluid. However, variations in phase-change rate in East Siberia corresponding to the 5–7 Myr long cycles of faster and slower subsidence alternating every 0.5 Myr cannot have been caused by temperature changes in the lower crust as these cycles are far shorter than the ~100 Myr characteristic time of lithospheric thermal relaxation. The absence of even minor crustal uplift above sea level rules out the rise of mantle plumes to the lithospheric base and the supply into the lower crust of water-bearing fluid they often carry. Then, only stresses in the lithosphere can have been subject to rapid and significant time-dependent changes. Deviatoric stresses may influence the gabbro-eclogite reaction rate and related subsidence, as well as fluid migration even in a “dry” lower crust. This mechanism is possibly common to many cratonic sedimentary basins.

The study was supported by grant 03-05-64166 from the Russian Foundation for Basic Research.

APPENDIX

POSSIBLE FORMATION MECHANISM OF ELEMENTARY CYCLES IN SECTIONS OF PERITIDAL FACIES

Sections of peritidal facies deposited in shallow water (≤ 10 m) are as a rule successions of meter-scale cycles [26, etc.], each started with a small rapid water-depth increase. These cycles are commonly thought to be of invariable duration which suggests their eustatic origin and relation of weak sea-level fluctuations to Milankovich cycles [12, 81]. Our study shows that the duration of Silurian elementary cycles in East Siberia varied in time and space, and their formation thus must have been controlled by factors other than eustasy. For instance, minor sea-depth changes associated with deposition discontinuity [78, 79, 82]. The rate of peritidal deposition can be dramatically changed by storms or sediment transport with irregular bottom currents, and is notably influenced by regional climate. Eustatic sea-level changes of the order of ≤ 1 m normally leave no imprint on sedimentation at ~10 m water depths, and some meter-scale cycles thus can be missed. The accommodation space produced by crustal subsidence becomes filled with sediments only partly, and the filled portion can vary from cycle to cycle. Anyway, synchronous chronozones provide reliable correlation of geographically dispersed sections, unlike the cycles of uncertain origin.

There is another factor often neglected. Fischer plots are commonly constructed assuming that cratonic crust experiences only slow tectonic subsidence at ~0.01–0.1 mm/yr. However, according to repeated leveling, slow general subsidence on cratons is overprinted with rapid uplift and subsidence up to a few millimeters per year or more [83, 84]. These rapid vertical movements, apparently within 1–10 m in magnitude, often change sign. The existence of brief episodes of crustal uplift and subsidence is also indicated by geomorphic evidence [86]. These low-magnitude but rapid tectonic movements can likewise be responsible for small 0.01–1.0 Myr changes in sea depths. This problem requires special consideration.

REFERENCES

1. Haq, B.U., J. Hardenbol, and P.R. Vail, Chronology of fluctuating sea levels since the Triassic, *Science*, **235**, 1156–1167, 1987.
2. Hallman, A. (ed.), *Phanerozoic sea level changes*, 266 pp., Columbia Univ. Press, New York, 1992.
3. Graciansky, P.C., J. Hardenbol, T. Jaquin, and P.R. Vail (eds.), *Mesozoic and Cenozoic sequence stratigraphy of European basins*, SEPM Special Publ., Series **60**, 786 pp., Tulsa, 1998.
4. Posamentier, H.W., and G.P. Allen, *Siliciclastic sequence stratigraphy — concepts and applications: SEPM concepts in sedimentology and paleontology*, SEPM, **7**, 204 pp., 2000.
5. Brekhuntsov, A.M., S.G. Ke-Kuha, V.N. Borodkin, and B.M. Blinov (eds.), *Proc. Geol. and Technol. Workshop “Exploratory drilling in Achimov section, East Urengoi zone”* [in Russian], 288 pp., Putived, Ekaterinburg, 1999.
6. Cooper, A., and G.S. Nowlan (eds.), *Proposed global stratigraphic section and point for base of the Ordovician system*, Intern. Working Group on the Cambrian-Ordovician boundary, Circular March, Calgary, 1999.
7. Maurer, F., Growth mode of middle Triassic carbonate platforms in the western Dolomites (Southern Alps, Italy), *Sedim. Geol.*, **134**, 275–286, 2000.

8. Cheng, D., M.E. Tucker, M. Jiang, and J. Zhu, Long-distance correlation between tectonic-controlled, isolated carbonate platforms by cyclostratigraphy and sequence stratigraphy in the Devonian of South China, *Sedimentology*, **48**, 57–78, 2001.
9. Dewey, J.F., and W.C. Pitman, Sea-level changes: Mechanisms, magnitudes and rates, in *Paleogeographic evolution and non-glacial eustasy, northern South America*, eds. J.L. Pindell and C.L. Drake, 1–17, SEPM Spec. Publ. 58, Tulsa, 1998.
10. Markwick, P.J., and D.B. Rowley, The geological evidence for Triassic to Pleistocene glaciations: Implications for eustasy, *Ibid.*, 17–45.
11. Miall, A.D., and C.F. Miall, Sequence stratigraphy as a scientific enterprise: The evolution and persistence of conflicting paradigms, *Earth Sci. Rev.*, **54**, 321–348, 2001.
12. Schwartzacher, W., Repetitions and cycles in stratigraphy, *Earth Sci. Rev.*, **50**, 51–75, 2000.
13. Webby, B.D., and J.R. Laurie (eds.), *Global perspectives on Ordovician geology*, 524 pp., Balkema, Rotterdam, 1992.
14. Artyushkov, E.V., M. Lindstrom, and L.E. Popov, The nature of transgressions and regressions in the Baltic paleobasin in the Cambrian and early Ordovician, *Dokl. RAN*, **357**, 5, 657–661, 1997.
15. Artyushkov, E.V., M. Lindstrom, and L.E. Popov, Relative sea-level changes in Baltoscandia in the Cambrian and early Ordovician: the predominance of tectonic factors and the absence of large scale eustatic fluctuations, *Tectonophysics*, **320**, 375–407, 2000.
16. Johnson, M.E., Stable cratonic sequences and a standard for Silurian eustasy, *Geol. Soc. Amer., Spec. Paper*, **306**, 202–211, 1996.
17. Artyushkov, E.V., and P.A. Chekhovich, Silurian deposition in East Siberia and the absence of large-scale eustatic fluctuations, *Geologiya i Geofizika (Russian Geology and Geophysics)*, **43**, 10, 893–915(839–862), 2002.
18. Tesakov, Yu.I., N.N. Predtechensky, A.Ya. Berger, L.S. Bazarova, O.K. Bogolepova, K.N. Volkova, M.M. Ignatovich, N.I. Kurushin, Yu.Ya. Latypov, T.V. Lopushinskaya, T.V. Mashkova, L.I. Sheshegova, A.P. Gubanov, E.A. Yolkin, N.M. Zaslavskaya, B.N. Zinchenko, E.O. Kovalevskaya, G.D. Kulik, T.A. Moskalenko, A.M. Obut, V.S. Pevzner, N.V. Sennikov, and G.A. Stukalina, *The Silurian type section of the Moyero River, Siberian Platform* [in Russian], 176 pp., Nauka, Novosibirsk, 1985.
19. Tesakov, Yu.I., N.N. Predtechensky, V.G. Khromykh, A.Ya. Berger, O.K. Bogolepova, K.N. Volkova, N.M. Zaslavskaya, N.I. Kurushin, V.A. Luchinina, T.A. Moskalenko, N.V. Sennikov, and A.G. Yadrenkina, *Silurian flora and fauna in Arctic regions of the Siberian Platform. New regional and local stratigraphic units* [in Russian], 216 pp., Nauka, Novosibirsk, 1986.
20. Tesakov, Yu.I., N.N. Predtechenskii, and V.G. Khromykh, Silurian stratigraphy of East Siberia, *Geologiya i Geofizika (Russian Geology and Geophysics)*, **39**, 10, 1335–1356(1338–1358), 1998.
21. Tesakov, Yu.I., N.N. Predtechensky, T.V. Lopushinskaya, V.G. Khromykh, L.S. Bazarova, A.Ya. Berger, and E.O. Kovalevskaya, *Stratigraphy of oil and gas basins of Siberia. Silurian of Siberian Platform*, 403 pp., GEO Branch, Izd. SO RAN, Novosibirsk, 2000.
22. Fischer, A.G., The Lofser cyclothems of the Alpine Triassic, *Kansas Geol. Surv. Bull.*, **169**, 107–149, 1964.
23. Goldhammer, R.K., P.J. Lehmann, and P.A. Dunn, The origin of high-frequency platform carbonate cycles and third-order sequences (Lower Ordovician El Paso GP, West Texas): Constraints from outcrop data and stratigraphic modeling, *J. Sedim. Petrol.*, **63**, 318–359, 1993.
24. Bosence, D.W.J., J.L. Wood, E.P.F. Rose, and H. Quing, Low- and high-frequency sea-level changes control, peritidal carbonate cycles, facies and dolomitization in the Rock of Gibraltar (Early Jurassic, Iberian Peninsula), *J. Geol. Soc. London*, **157**, 61–74, 2000.
25. Osleger, D.A., and J.F. Read, Relation of eustasy to stacking patterns of meter-scale carbonate cycles, Late Cambrian, U.S.A., *J. Sediment. Petrol.*, **61**, 1225–1252, 1991.
26. Wilson, J.L., *Carbonate facies in geological history*, 471 pp., Springer Verlag, Berlin, 1975.
27. Tesakov, Yu.I., N.N. Predtechenskii, V.G. Khromykh, A.Ya. Berger, T.K. Bazhenova, L.S. Bazarova, O.K. Bogolepova, Yu.A. Verkhovskiy, K.N. Volkova, A.P. Gubanov, N.M. Zaslavskaya, B.N. Zinchenko, A.B. Ivanovsky, E.O. Kovalevskaya, I.M. Kolobova, G.I. Korshunov, T.V. Lopushinskaya, N.V. Sennikov, G.A. Stukalina, A.E. Ukrainsky, and L.I. Sheshegova, *Silurian sections and fauna in the northern Tunguska basin* [in Russian], 193 pp., Nauka, Novosibirsk, 1992.
28. Gradstein, F.M., and J. Ogg, A Phanerozoic time scale, *Episodes*, **19**, 3–5, 1996.
29. Murphy, M.A., and A. Salvador (eds.), *International Stratigraphic Guide: an abridged version, Episodes* **22**, 255–271, 1999.

30. Johnson, J.G., G. Klapper, and Ch.A. Sandberg, Devonian eustatic fluctuations in Euroamerica, *Bull. Geol. Soc. Amer.*, **96**, 567–587, 1985.
31. Ross, C.A., and J.R.P. Ross, Late Paleozoic sea-levels and depositional sequences, *Spec. Publ. Cushman Foundations for Foraminiferal Research*, **24**, 137–149, 1987.
32. Odin, G.S., Geological time scale, *Serie II*, C. R. Acad. Sci., Paris, **318**, 59–71, 1994.
33. Harland, W.B., R.L. Armstrong, A.V. Cox, L.E. Craig, A.G. Smith, and D.G. Smith, *A geologic time scale*, 263 pp., Cambridge University Press, New York, 1990.
34. Sleep, N.H., Thermal effects of the formation of Atlantic continental margin by continental break up, *Geophys. J. Roy. Astron. Soc.*, **24**, 325–360, 1971.
35. McKenzie, D., Some remarks on the development of sedimentary basins, *Earth Planet. Sci. Lett.*, **40**, 25–32, 1978.
36. Peive, A.V. and A.L. Yanshin, *Tectonic map of northern Eurasia. Scale 1:5,000,000* [in Russian], GIN, Moscow, 1979.
37. Rosen, O.M., K.C. Condie, L.M. Natapov, and A.D. Nozhkin, Archean and Early Proterozoic evolution of the Siberian craton: A preliminary assessment, in *Archean crustal evolution*, ed. K.C. Condie, 411–459, Elsevier, Amsterdam, 1994.
38. Egor'kin, A.V., S.K. Zyuganov, N.I. Pavlenkova, and N.M. Chernyshov, Results of lithosphere studies from long-range profiles in Siberia, *Tectonophysics*, **140**, 29–37, 1987.
39. Pavlenkova, N.I., Crust and upper mantle structure in Northern Eurasia from seismic data, *Advances in Geophysics*, **37**, 1–133, 1996.
40. Haxby, W.F., D.L. Turcotte, and J.M. Bird, Thermal and mechanical evolution of the Michigan basin, *Tectonophysics*, **36**, 57–75, 1976.
41. Artyushkov, E.V. and M.A. Baer, Formation mechanism of petroliferous basins of the West Siberian Plate and Russian Platform, *Geologiya i Geofizika (Soviet Geology and Geophysics)*, **28**, 11, 25–36(20–31), 1987.
42. Artyushkov, E.V., *Physical tectonics* [in Russian], 458 pp., Nauka, Moscow, 1993.
43. Baird, D.J., J.H. Knapp, D.N. Steer, D.D. Brown, and K.D. Nelson, Upper-mantle reflectivity beneath the Williston basin, phase-change Moho, and the origin of intracratonic basins, *Geology*, **23**, 431–434, 1995.
44. Cloetingh, S., H. McQueen, and K. Lambeck, On a tectonic mechanism for regional sealevel variations, *Earth Planet. Sci. Lett.*, **75**, 157–166, 1985.
45. Nikishin, A.M., P.A. Ziegler, R.A. Stephenson, S.A.P.L. Cloetingh, A.V. Furne, P.A. Fokin, A.V. Ershov, S.N. Bolotov, M.V. Korotaev, A.S. Alekseev, V.I. Gorbachev, E.V. Shipilov, A.L. Lankreijer, E.Yu. Bembinova, and I.V. Shalimov, Late Precambrian to Triassic history of the East European craton: dynamics of sedimentary basin evolution, *Tectonophysics*, **268**, 23–63, 1996.
46. Artyushkov, E.V., Can the Earth's crust be in a state of isostasy? *J. Geophys. Res.*, **79**, 741–752, 1974.
47. Artyushkov, E.V., *Geodynamics* [in Russian], 328 pp., Nauka, Moscow, 1979.
48. Watts, A.B., The effective elastic thickness of the lithosphere and the evolution of foreland basins, *Basin Res.*, **4**, 169–178, 1992.
49. Burov, E.B., and M. Diament, The effective elastic thickness (T_e) of the continental lithosphere: What does it really mean? *J. Geophys. Res.*, **100**, 3095–3127, 1995.
50. Harper, J.F., Mantle flow and plate motions, *Geophys. J. Roy. Astron. Soc.*, **87**, 265–284, 1986.
51. Hager, B.H., and R.W. Clayton, Constraints on the structure of mantle convection using seismic observations, flow models, and the geoid, in *Mantle convection*, ed. W.R. Peltier, 657–766, Gordon and Breach, New York, 1989.
52. Burgess, P.M., M. Gurnis, and L.N. Moresi, Formation of sequences in the cratonic interior of North America by interaction between mantle, eustatic, and stratigraphic processes, *Bull. Geol. Soc. Amer.*, **109**, 1515–1535, 1997.
53. Sengör, A.M.J., B.A. Natal'in, and V.S. Burtman, Evolution of the Altaid tectonic collage and Paleozoic crustal growth in Eurasia, *Nature*, **364**, 299–307, 1993.
54. Ahrens, T.J., and G. Schubert, Gabbro-eclogite reaction rate and its geophysical significance, *Rev. Geophys. Space Phys.*, **13**, 383–400, 1975.
55. Austrheim, H., Influence of fluid and deformation on metamorphism of the deep crust and consequences for the geodynamics of collision zones, in *When continents collide: Geodynamics and geochemistry of ultrahigh-pressure rocks*, eds. B.R. Hacker and J.G. Liou, 297–323, Kluwer, Dordrecht, 1998.
56. Heinrich, C.A., Kyanite-eclogite to amphibolite facies evolution of hydrous mafic and pelitic rocks, Adula nappe, Central Alps, *Contrib. Miner. Petrol.*, **81**, 30–38, 1982.

57. Artyushkov, E.V., M.A. Baer, F.A. Letnikov, and V.V. Ruzhich, On the mechanism of graben formation, *Tectonophysics*, **197**, 95–115, 1991.
58. Makhotkin, I.L., D.Z. Zhuravlev, S.M. Sablukov, P.Yu. Zherdev, R.N. Thompson, and S.A. Gibson, Plume-lithosphere interaction: A geodynamic formation model for the Arkhangelsk diamond province, *Dokl. RAN*, **353**, 2, 1–5, 1997.
59. Artyushkov, E.V., and A.W. Hofmann, The neotectonic crustal uplift on the continents and its possible mechanisms: The case of Southern Africa, *Surv. Geophys.*, **19**, 515–544, 1998.
60. Saunders, A.D., J.G. Fitton, A.C. Kerr, M.Z. Norry, and R.W. Kent, The North Atlantic igneous province, *Geophys. Monogr.*, **100**, 45–92, 1997.
61. Pushkarev, Yu.D., A.M. Gottikh, A.M. Pisotsky, A.M. Zhuravlev, and A.M. Akhmedov, Isotope compositions of Sr, Pb, Nd, Os and REE distribution in oils, bitumens and black shales as indicators of matter sources, migration ways and genesis of hydrocarbon fluids, *Eighth Intern. Conference on Geochronology, Cosmochronology and Isotope Geology, Abstracts*, p. 257, Berkley, 1994.
62. Pisotsky, B.I., *Processes of reducing fluidization in petroleum provinces and the role of mantle components in hydrocarbon genesis* [in Russian], ScD Thesis, 357 pp., VNIIGeosistem, Moscow, 1999.
63. Gottikh, R.P., B.I. Pisotsky, and D.Z. Zhuravlev, Geochemistry of bitumens and oils in some petroleum provinces: Nd and Sr isotope ratios, *Dokl. RAN*, **375**, 1, 83–88, 2000.
64. Yudovich, Ya.E., and M.P. Ketris, *Geochemistry of black shales* [in Russian], 272 pp., Nauka, Leningrad, 1988.
65. Nelson, D.R., Isotopic characteristics of potassic rocks: Evidence for the involvement of subducted sediments in magma, *Lithos*, **28**, 403–420, 1992.
66. Taylor, S.R., and S.M. McLennan, *The continental crust: Its composition and evolution*, 312 pp., Blackwell Scientific, Boston, 1985.
67. Gibbs, J.W., The Collected Works of J. Willard Gibbs, *Thermodynamics*, vol. 1, 55–349, Longmans, Green and Co., New York, 1928.
68. Rebinder, P.A., and E.K. Wenstrom, The effect of medium and adsorption layers on plastic flow of metals, *Izv. OMEN. Ser. Fiz.*, 4/5, 531–550, 1937.
69. Ghienne, J.-F., Late Ordovician sedimentary environments, glacial cycles, and post-glacial transgression in the Taoudeni Basin, West Africa, *Palaeogeography, Palaeoclimatology, Palaeoecology*, **189**, 117–145, 2003.
70. Alekseev, V.B., Structural paragenesis in zones of stress metamorphism, *Geotektonika*, 5, 21–32, 1990.
71. Jamteveit, B., K. Bucher-Nurminen, and H. Austrheim, Fluid controlled eclogitization of granulites in deep crustal shear zones. Bergen arcs, Western Norway, *Contrib. Miner. Petrol.*, **104**, 184–193, 1990.
72. Zoback, M.L., First- and second-order patterns of stresses in the lithosphere: the World Stress Map Project, *J. Geophys. Res.*, **97**, 11,703–11,728, 1992.
73. Milanovsky, E.E., Phase correlation of high-frequency geomagnetic reversals, eustatic sea-level fall, and increase in compressional crustal strain in the Mesozoic and Cenozoic, *Geotektonika*, 1, 3–11, 1996.
74. Bankwitz, P., and E. Bankwitz, Einige Merkmale tectonischer Erdkrustbewegungen im Hinblick auf rezente Bewegungen, *Gewel. Geophys. Veroff.*, **B3**, 35, 110–118, 1974.
75. Likhachev, V.A., and V.G. Malinin, *Structural-analytical theory of strength* [in Russian], 471 pp., Nauka, St. Petersburg, 1993.
76. Traskin, V.YU., A.G. Bedarev, Z.N. Skvortsova, L.G. Arutyunyan, L.S. Bryukhanova, and N.V. Pertsov, Inter-crystallite destruction of polycrystals of alkali halogenides with interstitial fluids, *Dokl. AN USSR, Ser. B.*, 11, 48–51, 1986.
77. Miall, A.D., The Exxon global cycle chart: An event for every occasion, *Geology*, **20**, 787–790, 1992.
78. Drummond, C.N., and B.H. Wilkinson, Aperiodic accumulation of peritidal carbonates, *Geology*, **21**, 1023–1026, 1993.
79. Burgess, P.M., V.P. Wright, and D. Emery, Numerical forward modelling of peritidal carbonate parasequence development: Implications for outcrop interpretation, *Basin Res.*, **13**, 1–25, 2001.
80. Pope, M., and J.F. Read, Ordovician metre-scale cycles: Implications for climate and eustatic fluctuations in the central Appalachians during a global greenhouse, non-glacial to glacial transition, *Palaeogeography, Palaeoclimatology, Palaeoecology*, **138**, 27–42, 1998.
81. Gale, A.S., J. Hardenbol, B. Hathway, W.J. Kennedy, J.R. Young, and V. Phansalkar, Global correlation of Cenomanian (Upper Cretaceous) sequences: Evidence for Milankovitch control on sea level, *Geology*, **30**, 4, 291–294, 2002.
82. Ginsburg, R.N., Landward movement of carbonate mud: new model for regressive cycles in carbonates (abstract), *Amer. Assoc. Petrol. Geol. Bull.*, **55**, p. 340, 1971.

83. Meshchersky, I.N. (coordinator), *Map of recent vertical crustal movements in the territory of Bulgaria, Hungary, GDR, Poland, Romania, European USSR, and Czechoslovakia. Scale 1:2,500,000* [in Russian], GUGK, Moscow, 1986.

84. Kashin, L.A., *Map of recent vertical crustal movements in the territory of USSR, from geodetic data. Scale 1:5,000,000* [in Russian], GUGK, Moscow, 1989.

85. Belousov, V.V. *Basic problems in geotectonics* [in Russian], 608 pp., Gosgeoltekhizdat, Moscow, 1962.

86. Kaftan, V.I., and L.I. Serebryakova, Geodetic methods for geodynamic problems (Recent vertical crustal movements), *Bull. VINITI. Ser. Geodez. i Aeros'yomka*, 28, 152 pp., 1990.

Editorial responsibility: V.V. Reverdatto

Received 12 May 2003